

NN17

Effect of Isothermal Heat Treatment on Cyclic Life of Ytria Stabilized Zirconia and Gadolinium Zirconate Thermal Barrier Coating

AD Johari^a, SM Yunus^b, SA Biyamin^b, MM Rahman^c, H Hasini^c, A Manap^{c*}

^aTNB Repair and Maintenance Sdn Bhd, Jalan Dato Mohd Sidin, 41000 Klang, Malaysia

^bTNB Research Sdn Bhd, No. 1, Kawasan Institusi Penyelidikan, Jalan Ayer Itam, 43000 Kajang, Malaysia

^cUniversiti Tenaga Nasional, Department of Mechanical Engineering, College of Engineering, 43000 Kajang, Malaysia

Abstract

The effect of isothermal heat treatment on the thermal cyclic life of yttria stabilized zirconia (YSZ) and gadolinium zirconate (GZ) thermal barrier coatings (TBCs) have been investigated. The purpose of the isothermal heat treatment is to simulate thermal exposure on the TBC in the gas turbine. Duplex YSZ TBC with YSZ as a topcoat and NiCrAlY as a bondcoat and five-layered GZ TBC with GZ as the topcoat (GZ / 50 wt.%GZ+50 wt.%YSZ / YSZ / 50 wt.%YSZ+50 wt.% NiCrAlY / NiCrAlY) were plasma sprayed onto Nimonic 263 substrates to a total thickness of 900 μ m using F4-MB gun. The isothermal heat treatment was performed at a temperature of 1100°C for 100 hours with a heating rate of 250°C/hour in an air furnace. The thermal cyclic tests were performed with the following cycle in an air furnace: heat up from 1000°C to 1200°C within 1 hour, dwell at 1200°C for 5 minutes, water quench and oven dry. The cycle is repeated until 20% spallation of the coating. Result indicates that the isothermally heat treated five-layered GZ TBC has a better cyclic life than the duplex YSZ TBC and as-sprayed GZ TBC.

© 2018 Elsevier Ltd. All rights reserved.

Selection and/or Peer-review under responsibility of 14th International Conference on Nanosciences & Nanotechnologies (NN17).

Keywords: Gadolinium zirconate; YSZ; TBC; five-layered; functionally graded

* Corresponding author. Tel.: +603-8921 2020; fax: +603-8921 2113.

E-mail address: abreeza@uniten.edu.my

Nomenclature

BC	Bondcoat
EDS	Energy dispersive spectroscopy
GZ	Gadolinium Zirconate
REZ	Rare Earth Zirconate
TGO	Thermally grown oxide
YSZ	Yttria stabilized zirconia

1. Introduction

In the 70's, the turbine inlet temperature of a typical gas turbine was approximately 900°C. In recent year, the turbine inlet temperature has increased to 1380°C. Gas turbine manufacturers are continue making high-efficiency turbine by changing to better material, designing better cooling flow and applying insulation layers onto hot surfaces of GT component [1, 2]. This insulation layer is called Thermal Barrier Coating (TBC).

As gas turbine operating temperature increases, a high-temperature phenomenon such as oxidation, corrosion, and creep lead to material failure. Gas turbine material is manufactured from state-of-the-art superalloys, and they are already at their maximum potential. Superalloy development seems to reach its plateau and a further increase in operating temperature cannot be relied on superalloy development only.

As gas turbine operating temperature increases, extra work is needed to provide the flow of cooling air to bring the gas turbine materials below their maximum operating limit. The extra work in delivering cooling air affects the efficiency of the gas turbine due to its inability to withstand high temperature. TBC mitigates the superalloy limitation by providing a temperature gradient between the hot gas stream and the component surfaces. TBC typically reduces metal temperature by 4-9°C/25µm of TBC thickness [2]. The lower metal temperature allows gas turbine designer to either reduce the cooling air to raise efficiency and save fuel, or increase the turbine inlet temperature and increase powder or retain the same flow of cooling air and improve component durability.

The current TBC system consists of metallic bondcoat and yttria stabilized zirconia (YSZ) ceramic topcoat. It suffers from some limitations. Firstly, the YSZ suffers from sintering effect at a temperature above 1200°C, which causes its insulation property to deteriorate [3]. Secondly, YSZ has a high oxygen permeability, which allows thermally grown oxide layer (TGO) to form in between bondcoat and YSZ layers and within bondcoat [4]. While the TGO is beneficial to reduce the rate of oxidation, a thick TGO leads to spallation of YSZ layer and causes TBC to fail.

Therefore, tomorrow's gas turbine requires a new TBC material that is stable at high temperature, has better thermal resistance than YSZ, good thermal cyclic performance, and low oxygen permeability [5]. Rare earth zirconate (REZ) has been found to have high-temperature stability, better thermal resistance than YSZ and low oxygen permeability [3, 6]. However, it has poor thermal cyclic performance due to the low coefficient of thermal expansion (CTE) and causes CTE mismatch with bondcoat. Functionally graded TBC is a method proposed to manage high stress caused by low CTE of the top layer [7–9]. Functionally graded TBC works by adding intermediate layer or layers between the top layers and bondcoat. The architecture reduces thermal stress between the top layer and bondcoat and thus reduce risks of coating spallation. Double ceramic layer (DCL) and five-layered TBC are examples of functionally graded TBC.

Therefore, the aim of this work is to investigate the effect of isothermal heat treatment on the cyclic life time of gadolinium zirconate TBC and compare the result with YSZ TBC. In this study, the YSZ TBC was applied as duplex layer while GZ TBC was applied as five-layered system as shown in Fig. 1.

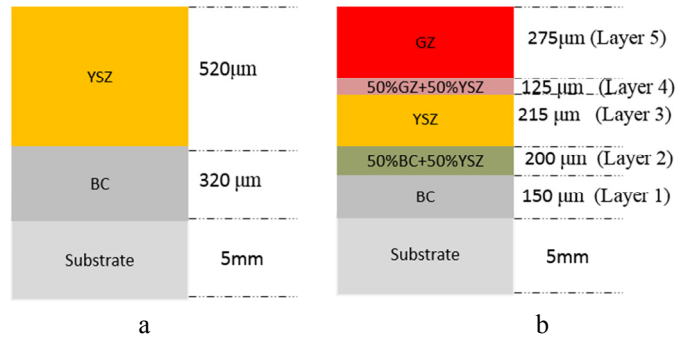


Fig. 1 (a) Duplex YSZ TBC; (b) five-layered GZ TBC

2. Experimental procedures

2.1. Preparation of powder mixture

Layer 2 of GZ TBC were sprayed using 50% of NiCrAlY powder (Oerlikon Metco Amdry 962) and 50% of YSZ powder (Oerlikon Metco 204G-XCL) while layer 4 of GZ TBC were sprayed using 50% of YSZ powder and 50% of GZ powder (57%Gd₂O₃ 43%ZrO₂, Transtech Inc, Adamstown, MD, USA). The powder mixtures were agitated for 4 hours in a powder tumbler to ensure homogeneity.

2.2. Coating Preparation

All coatings were plasma sprayed by a plasma system (MP-100 multicoating system Flame Spray Technologies BV) using F4-MB gun with 6 mm diameter nozzle. 1 inch diameter specimens were cut from Nimonic 263 (High Temp Metal Inc, Sylmar, Ca) alloy plate of 5 mm thickness. The nominal composition of the Nimonic 263 is given in Table 1.

Table 1 Chemical composition of Nimonic 263 in wt.%

Ni	Cr	Co	Mo	Ti	Fe	Al	Mn	Bal
51.0	20.1	19.3	5.9	2.2	.6	.43	.33	.14

The specimens were grit blasted with aluminium oxide mesh 24 and compressed air at 6 bar to enhance adhesion. The coating powders were dried in an oven at 120 °C for 2 hours. Then, NiCrAlY, 50% NiCrAlY+50%YSZ, YSZ, 50%YSZ+50%GZ, and GZ coating were deposited into Nimonic 263 substrate to fabricate five-layered GZ TBC. The duplex YSZ TBC was applied using NiCrAlY and YSZ coating. The thermal spray parameter is given in **Error! Not a valid bookmark self-reference.** Six samples are prepared for each type of coatings.

Table 2 Parameters used for plasma spraying

	Layer 1 (BC)	Layer 2	Layer 3 (YSZ)	Layer 4	Layer 5
Current, A	550	560	575	585	550
Primary gas (Ar), NLPM	55	45	35	35	35
Secondary gas (H ₂), NLPM	9.4	9.7	10	9	8
Carrier gas (Ar), NLPM	4	3.5	3	2.7	2.7
Disc, %	7.5	25	42	33	33
Powder feed rate, g/min	40	50	60	47	47
Stirrer, %	40	60	85	85	85

2.3. Microstructure of TBC

Specimen was cross-sectioned. The specimen was cut with an abrasive cutting tool (Discotom 5, Struers). The blade was made to cut into the coating to avoid coating spallation. The cut section was then mounted into Struers epoxy set which consists of a mixture of 10:1 (resin: hardener). The mixture was poured into a standard circular metallographic mold and allowed to cool for 12 hours. The epoxy mount holds the cut specimen so that further grinding and polishing can be done effectively.

After curing, the mounted sample was hand ground and polished on rotating polishing machine with 200 mm diameter disc (Tegramin 20, Struers) Disposable Struers silicon carbide grinding disc were used in a 120, 320, and 1000 grit sizes progression to polish the sample. Water was used as a coolant during grinding stages. Struers diamond grit polishing suspension was used to polish the sample. The grit size of the polishing suspension was 9 μm , 3 μm , and 1 μm . Multiple polishing pads (MD-Largo, MD-Mol, and MD-Nap, Struers) were used during each of the polishing stages. The sample was rinsed with deionized water between polishing stages to avoid cross contamination of polishing suspensions.

The samples were observed using Field Emission Scanning Electron Microscope (FE-SEM) (Hitachi SU 8020) using 15kV accelerating voltage. Several cross-sectional micrographs were taken for TBC thickness measurement and porosity measurement. Three SEM micrographs were used for porosity measurement using ImageJ software [10]. In each image, three areas were chosen for porosity measurement. The threshold was left on automatic to ensure minimal user intervention. The average value was reported as porosity measurement. Based on SEM micrographs taken after isothermal heat treatment, TGO thickness was measured on each cross-sectional SEM at 6 to 13 different locations and the average value was reported as TGO thickness.

2.4. Isothermal heat treatment

Three samples from YSZ TBC and GZ TBC respectively were isothermal heat treated in an air furnace at 1100 °C for 100 hours. After 100 hours, the specimens were left in the furnace to cool to room temperature.

2.5. Thermal cyclic test

The thermal cyclic test was performed by heating in air furnace and water quenching method. The samples were put in air furnace and were heated from 1000 °C to 1200 °C within an hour, dwell at 1200 °C for 5 minutes, then they were cooled in running water bath with temperature of 25 °C. When the samples were cooled to room temperature, they were taken out, oven dried and put in to the air furnace to repeat the same process. When 20% of the coating surface was peeled off or cracked (based on visual inspection using naked eyes), the process was stopped and the number of cycle was recorded as thermal cyclic life of the coating. The average value of 3 samples was reported as thermal cyclic life. The macro images of the damaged samples were captured using digital camera.

3. Results and discussion

3.1. Microstructure of TBC

Fig. 2 displays the cross sectional morphology of the YSZ TBC and GZ TBC of the as-sprayed coatings and as-oxidized coatings. A certain quantity of pores and micro-cracks can be observed. The microstructure of YSZ can easily distinguishable between YSZ and bond coat layers. The five-layered GZ TBC is quite difficult to distinguished between layers, particularly, in the as-sprayed coating and thus, required energy dispersive spectroscopy (EDS) to identify element within the coating.

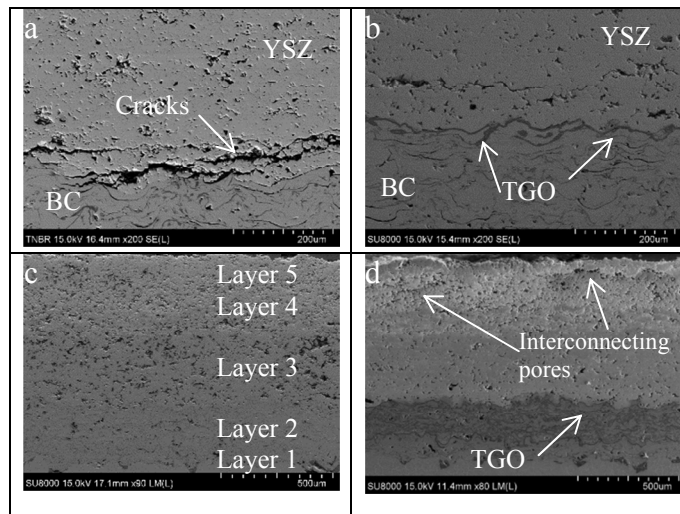


Fig. 2 Cross sectional morphology a) YSZ TBC as-sprayed b) YSZ TBC oxidized c) GZ TBC as-sprayed d) GZ TBC oxidized.

Using image analyser (ImageJ) to analyse the SEM micrograph, the average porosity of the topmost layer were measured and presented in Fig. 3. Similar to Parlayigit et al. [11] finding, the porosity of YSZ layer decrease after isothermal heat treatment of 1100°C for 100 hours. However, the porosity of top layers GZ TBC increase after isothermal heat treatment. The increase of porosity could be contributed by the existence of interconnecting pores or microcrack within the top layer after isothermal heat treatment as shown in Fig. 2. As the porosity measurement was carried out using image analyzer, the software was unable to differentiate between pores and microcrack and thus, causing the porosity percentage to increase. Upon closer inspection on porosity at layer 3 and layer 4 of GZ TBC as shown in Fig. 4, it was found that porosity at the layer 3 (YSZ layer) reduced after isothermal heat treatment, similar to YSZ TBC. GZ TBC has YSZ porosity reduction of 27.9% while YSZ TBC has a porosity reduction of 46.3%. Since layer 3 and layer 4 of GZ TBC were sprayed with similar YSZ powder, this finding shows that the addition of layer 4 and layer 5 would reduce the sintering effect on YSZ. Based on SEM micrograph of the heat treated samples, the average TGO thickness after isothermal heat treatment is 3.93 μm and 4.61 μm for YSZ and GZ TBC respectively and thus, not detrimental to the TBC because the topcoat would only start delaminated if TGO thickness greater than 10 μm [12].

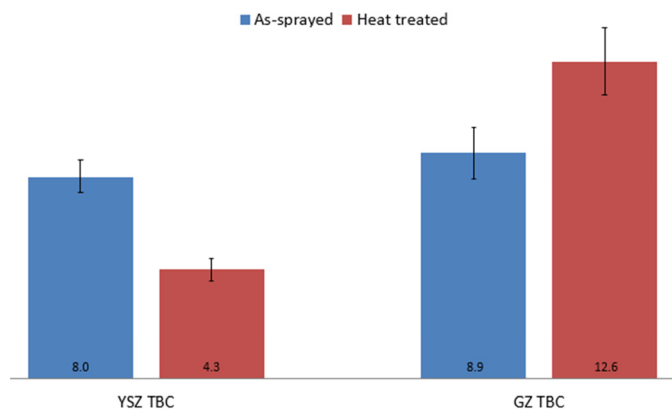


Fig. 3 Percentage porosity of top layer of YSZ TBC and GZ TBC

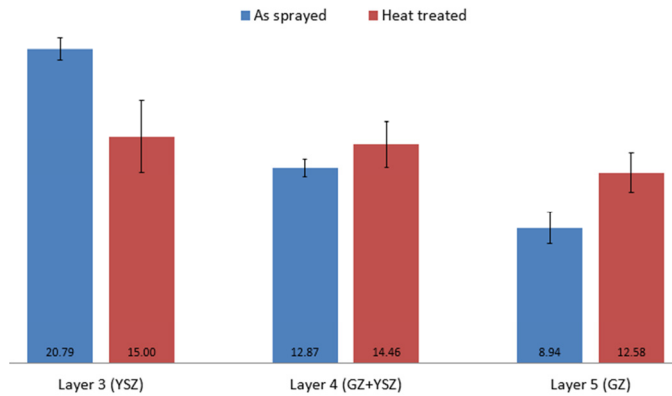


Fig. 4 Percentage porosity in layer 3, 4 and 5 of GZ TBC.

3.2. Thermal cyclic life

Fig. 5 shows the thermal cyclic lifetime of YSZ TBC and GZ TBC at 1200 °C. It can be seen that five-layered GZ TBC has a longer thermal cyclic lifetime in both as-sprayed and heat treated condition in comparison to YSZ TBC. The result is in agreement with L. Wang et al. [13] who obtained a thermal cyclic improvement of 600% using DCL lanthanum zirconate (a rare earth zirconate) as compared to standard YSZ. The low thermal cyclic life of YSZ TBC could be explained by its relatively low porosity especially after heat treatment. Myoung et al. [12] demonstrated that low porosity YSZ coating has low thermal cyclic life. In addition, the relatively thick (500 μm) of YSZ layer also affecting the thermal cyclic life and the result is in good agreement with Khan et al. who obtained 3 to 4 cycles for 500 μm thick YSZ layer using furnace heating and water quench method [14].

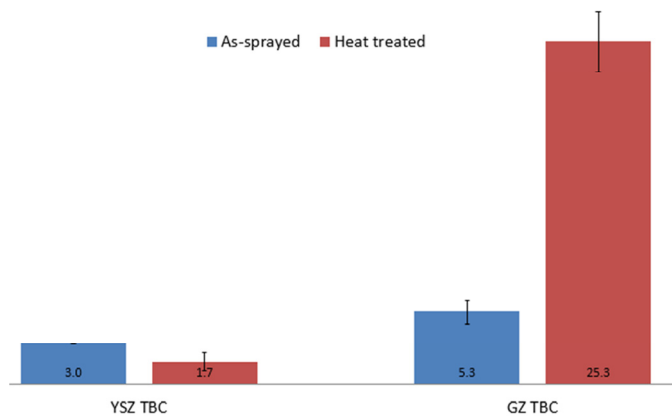


Fig. 5 Thermal cyclic life of YSZ TBC and GZ TBC

In general, TBC failure is associated with the build-up of stress mainly from oxide scale growth and CTE mismatch. During the thermal cyclic process, coating specimen was taken out from the furnace at 1200 °C and immediately quenched in water. This process developed a very high stress in the coating due to the difference in CTE between ceramic layers, TGO and base metal. Table 3 shows the average value of CTE is in the order of BC > YSZ > GZ > TGO (Al₂O₃).

Five-layered GZ TBC has the highest thermal cyclic life. It performed better than YSZ coatings by 70% in as-sprayed condition. In the previous work, the five-layered coating was 43% better than duplex YSZ in as-sprayed condition [6]. It shows that five-layered coating can endure stress induced during the thermal cyclic test. After heat

treatment, GZ TBC performed exceptionally well in comparison to other low porosity YSZ coating by 1388%. The exceptional improvement could be contributed to the increase in porosity within layer 4 and layer 5 which increase their strain tolerances and are able to compensate extreme stress caused by the thermal cyclic test.

Table 3 Properties of TBC layers and nickel alloy

	Melting Temp. °C	Operating Temp. °C	CTE at 30 – 1000°C, 10-6K	Thermal conductivity at 1000°C, W/mK	Density, g/cm ³
Nickel alloy	1300	1150	13.3	13.4	8.15
MCrAlY (BC)		1050	12	12.5	7.8
YSZ	2680	1200	11.5	2.12	5.9
GZ	2300	1650	10.4	1.6 (at 800°C)	7.0
TGO			8		

Reference: [15–20]

3.3. Thermal cyclic failure mechanism

The surface morphology of the coatings after thermal cyclic test at 1200 °C are shown in Fig. 6. Failure began from the edges of the samples and then propagated to the adjacent areas. The failure started from the edges because of the extreme heating and cooling condition caused thermal stresses at the edges. Other studies have also mentioned the edge effect during thermal cyclic test [21, 22]. The YSZ specimens failed at the bondcoat / topcoat interface as shown in Fig. 6 (a) and (b). The failure for five-layered GZ TBC began from the layer 5 (topmost), then propagate to the center and into the layer 4 and the layer 3 as shown in Fig. 6 (c) and (d). After the samples failed, the center area of the coating still adhered to the substrate perfectly.

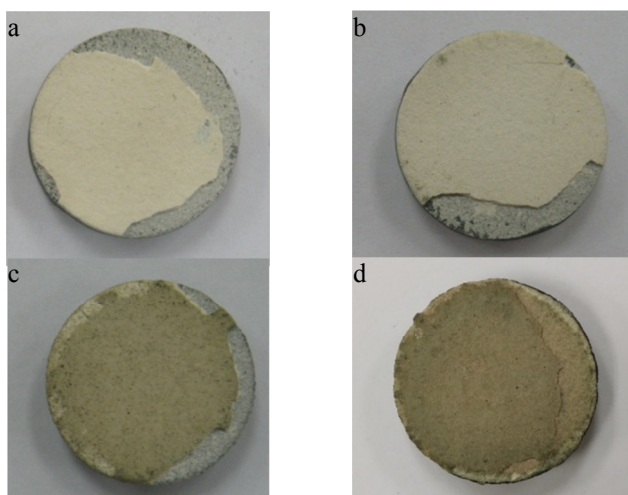


Fig. 6 The macrograph of coating after thermal shock test at 1200 °C. (a) YSZ TBC as sprayed condition (3 cycles); (b) YSZ TBC as heat treated condition (1 cycle); (c) GZ TBC as sprayed condition (4 cycles); (d) GZ TBC as heat treated condition (21 cycles)

The cross sectional micrographs of YSZ TBC (as sprayed condition) after thermal cyclic are shown in Fig. 7. The YSZ layer spalled from the bondcoat and some vertical cracks and horizontal cracks occurred within the YSZ layer. Only minor horizontal cracks occurred within the bondcoat. In addition, the interface between YSZ / bondcoat is still intact. There is no chipping spallation observed on the coating surface, indicating that the sintering of the YSZ layer is not the failure mechanism for the coating [23]. Based on Fig. 2 (a), horizontal crack within the YSZ layer

and near to bond coat was already displayed in the as sprayed condition. The crack most probably occurred due to residual stresses during plasma spray application. The thermal cyclic process exaggerated the stresses within the coating and the coating failed at the weakest area. Therefore, the main failure mechanism for this coating are stress due to CTE mismatch and cracks that occurred due to residual stress during coating application.

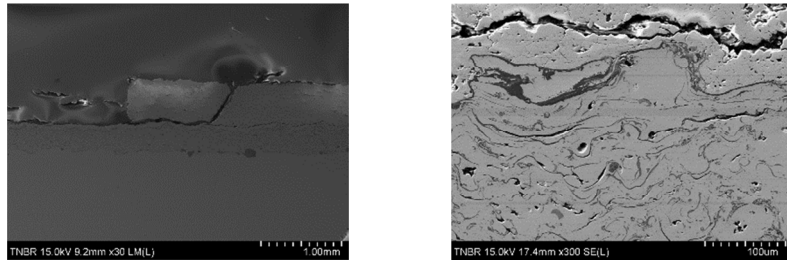


Fig. 7 Cross section micrograph of YSZ coating (as-sprayed) after thermal cyclic (3 cycles)

The cross sectional micrographs of YSZ TBC (heat treated condition) after thermal cyclic are shown in Fig. 8. The YSZ layer spalled from the bondcoat and some vertical cracks and horizontal cracks occurred within the YSZ layer. Only minor horizontal cracks occurred within the bondcoat. In addition, the interface between YSZ / bondcoat is still intact. There is no chipping spallation observed on the coating surface, indicating that the sintering of the YSZ layer is not the failure mechanism for the coating. Based on Fig. 2 (b), the horizontal crack within YSZ near the bond coat seemed to be ‘healed’ after isothermal heat treatment, leaving a narrow trace of horizontal crack. The isothermal heat treatment densitized the coating and close up gap. However, the thermal cyclic test proved that isothermal heat treatment won’t heal the crack and stresses from thermal cyclic could still induce the crack resulting in coating failure. Therefore, the main failure mechanism for this coating are stress due to CTE mismatch and existing cracks that occurred due to residual stress during coating application.

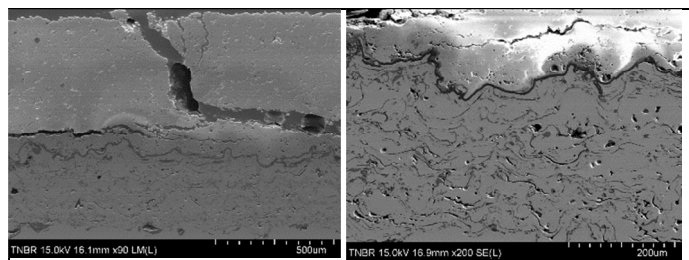


Fig. 8 Cross section micrograph of YSZ coating (heat treated) after thermal cyclic (1 cycle)

The cross sectional micrographs of five-layered GZ TBC (as-sprayed) after thermal cyclic are shown in Fig. 9. There are horizontal cracks at the interface of layer 2 (YSZ+MCrAlY) and layer 3 (YSZ) and vertical cracks from layer 5 to layer 3. There is evident of TGO within layer 1 and layer 2 but no crack within these layers. Based on Fig. 2 (c), there is no crack within YSZ layer in the as-sprayed condition. However, the YSZ layer has relatively high porosity. There is no chipping spallation observed on the coating surface, indicating that the sintering of the GZ layer is not the failure mechanism for the coating. The major failure took place at the interface of layer 2 and layer 3, indicating that the failure was due to the bondcoat oxidation and not by the limited sintering ability of GZ layer. There was evident of CSN cluster within the TGO obtained using EDS (Fig. 10) which increased the TGO volume and caused high stresses within the coating. Since it was difficult to distinguish $(Cr, Al)_2O_3$ from $Ni (Cr, Al)_2O_4$ (CSN cluster), it was assumed that oxides containing $<8\%$ mol.% Ni+Co and $>35\%$ mol.% Al+Cr were $(Cr, Al)_2O_3$, as $NiAl_2O_4$ containing 13-16 mol.% Ni and 27-30 mol.% Al [24]. The result was expected because CSN cluster could only be formed if the bondcoat temperature was higher than $1100\text{ }^\circ\text{C}$ [25]. Therefore, the main failure mechanism for this coating was stresses due to bondcoat oxidation.

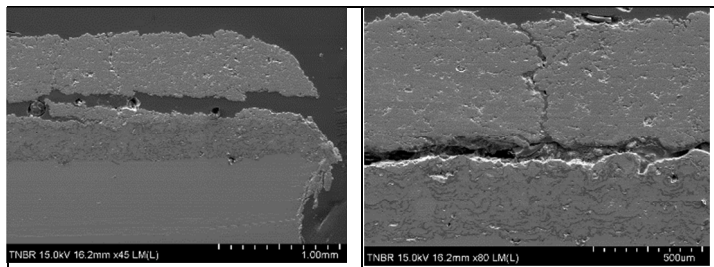


Fig. 9 Cross section micrograph of five-layered GZ coating (as-sprayed) after thermal cyclic (4 cycles)

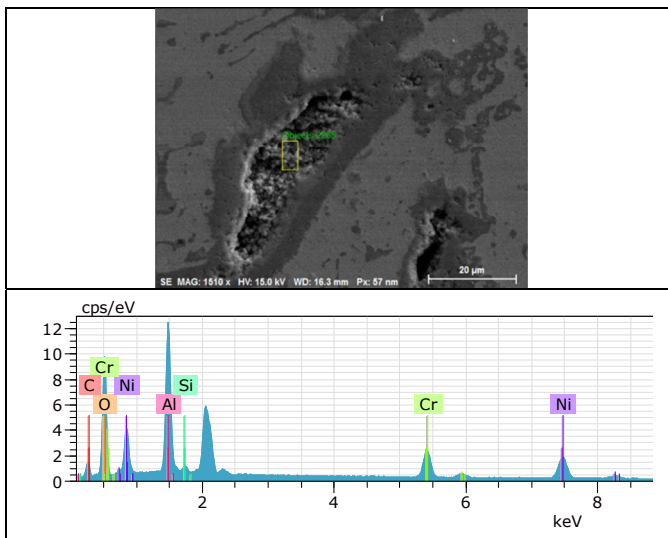


Fig. 10 EDS analysis from TGO of five-layered GZ coating (as sprayed) after thermal cyclic (4 cycles).

The cross sectional micrographs of five-layered GZ TBC (heat treated) after thermal cyclic are shown in Fig. 11. There is no horizontal crack at the interface between layer 3 and layer 2. Based on Fig. 2 (d), there were interconnecting pores within layer 5. During thermal cyclic process, the pores became crack and peel off due to thermal stresses. The existence of vertical cracks from layer 5 to layer 3 also indicated that there were still stresses within the coating which has to be relaxed through formation of these vertical cracks. Nevertheless, the coating withstood 21 cycles without massive failure. This shows the excellent thermal cyclic resistance of five-layered GZ TBC.

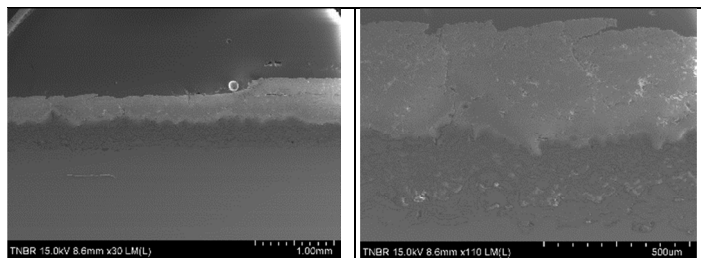


Fig. 11 Cross section micrograph of five-layered GZ coating (heat treated) after thermal cyclic (21 cycles)

4. Conclusion

In this study, two types of TBCs; duplex YSZ and five-layered GZ have been deposited on superalloy of Nimonic 263 substrates. Both coatings were deposited via air plasma spray (APS) process. The TBC samples were subjected to as sprayed condition and isothermal heat treatment test that was carried out at 1100 °C for 100 hours. The isothermal heat treatment improved thermal cyclic lifetime of five-layered GZ TBC by more than five-fold in comparison to the as-sprayed coatings. The probably reason was the ability of heat treated five-layered GZ TBC to release stresses within the coating which were contributed by thermal spray process, CTE mismatch and TGO. The failure of YSZ TBC after isothermal heat is believed mainly due to its inability to absorb stresses caused during thermal cyclic test and pre-existing cracks due to residual stress from thermal spray application.

Acknowledgements

The authors would like to thank Tenaga Nasional Berhad (TNB) for the financial aid and special thanks to the Materials Group of TNB Research Sdn Bhd and TNB REMACO Repair Center for their full cooperation in this work.

References

- [1] Z. Huda, T. Zaharinie, and H. A. Al-ansary, *Int. J. Mech. Mater. Eng.*, pp. 1–12, 2014.
- [2] P. W. Schilke, “Advanced Gas Turbine Materials and Coatings,” *GE Energy*, 2004..
- [3] K. Bobzin, N. Bagcivan, T. Brögelmann, and B. Yildirim, *Surf. Coatings Technol.*, vol. 237, pp. 56–64, Dec. 2013.
- [4] A. Keyvani, *J. Alloys Compd.*, vol. 623, pp. 229–237, 2015.
- [5] G. Di Girolamo, C. Blasi, A. Brentari, and M. Schioppa, *Energia, Ambient. e Innov.*, no. 1–2/2013, pp. 69–76, 2013.
- [6] C. S. Ramachandran, V. Balasubramanian, P. V. Ananthapadmanabhan, and V. V., *Ceram. Int.*, vol. 38, no. 5, pp. 4081–4096, Jul. 2012.
- [7] W. Y. Lee, D. P. Stinton, C. C. Berndt, S. Brook, and N. York, “Concept of Functionally Graded Materials for Advanced Thermal Barrier Coating Applications,” no. 191958, 1996.
- [8] H.-P. Xiong, A. Kawasaki, Y.-S. Kang, and R. Watanabe, *Surf. Coatings Technol.*, vol. 194, no. 2–3, pp. 203–214, May 2005.
- [9] K. Kokini, J. DeJonge, S. Rangaraj, and B. Beardsley, *Surf. Coatings Technol.*, vol. 154, no. 2–3, pp. 223–231, May 2002.
- [10] G. Dwivedi, Y. Tan, V. Viswanathan, and S. Sampath, *J. Therm. Spray Technol.*, vol. 24, no. 3, pp. 454–466, 2015.
- [11] A. S. Parlakyigit and A. C. Karaoglanli, *Acta Phys. Pol. A*, vol. 125, no. 2, pp. 232–234, 2014.
- [12] S. W. Myoung, S. S. Lee, H. S. Kim, M. S. Kim, Y. G. Jung, S. Il Jung, T. K. Woo, and U. Paik, *Surf. Coatings Technol.*, vol. 215, pp. 46–51, 2013.
- [13] L. Wang, Y. Wang, X. G. Sun, J. Q. He, Z. Y. Pan, and C. H. Wang, *Ceram. Int.*, vol. 38, no. 5, pp. 3595–3606, Jul. 2012.
- [14] A. N. Khan and J. Lu, *Surf. Coatings Technol.*, vol. 201, no. 8, pp. 4653–4658, 2007.
- [15] M. Han, G. Zhou, J. Huang, and S. Chen, *Surf. Coatings Technol.*, vol. 236, pp. 500–509, Dec. 2013.
- [16] R. Vaßen, M. O. Jarligo, T. Steinke, D. E. Mack, and D. Stöver, *Surf. Coatings Technol.*, vol. 205, no. 4, pp. 938–942, Nov. 2010.
- [17] X. Zhong, H. Zhao, X. Zhou, C. Liu, L. Wang, F. Shao, K. Yang, S. Tao, and C. Ding, *J. Alloys Compd.*, vol. 593, pp. 50–55, Apr. 2014.
- [18] H. Lehmann, D. Pitzer, G. Pracht, R. Vassen, and D. Sto, *J Am Chem Soc*, vol. 86, no. 186991, pp. 1338–1344, 2003.
- [19] A. S. M. Ang and C. C. Berndt, *Int. Mater. Rev.*, vol. 59, no. 4, pp. 179–223, 2014.
- [20] A. Keyvani, M. Saremi, and M. H. Sohi, *J. Alloys Compd.*, vol. 509, no. 33, pp. 8370–8377, Aug. 2011.
- [21] H. Jamali, R. Mozafarinia, R. Shoja Razavi, and R. Ahmadi-Pidani, *Ceram. Int.*, vol. 38, no. 8, pp. 6705–6712, 2012.
- [22] R. Ghasemi, R. Shoja-razavi, R. Mozafarinia, and H. Jamali, *Ceram. Int.*, vol. 40, no. 1, pp. 347–355, 2014.
- [23] H. Dong, D. Wang, Y. Pei, H. Li, P. Li, and W. Ma, *Ceram. Int.*, vol. 39, no. 2, pp. 1863–1870, 2013.
- [24] W. R. Chen, X. Wu, B. R. Marple, D. R. Nagy, and P. C. Patnaik, *Surf. Coatings Technol.*, vol. 202, pp. 2677–2683, 2008.
- [25] C. H. Lee, H. K. Kim, H. S. Choi, and H. S. Ahn, *Surf. Coatings Technol.*, vol. 124, no. 1, pp. 1–12, Feb. 2000.